PERFORMANCE OF ULTRASONIC IMAGING WITH FREQUENCY DOMAIN SAFT (F-SAFT)

D. Lévesque, A. Blouin, C. Néron, and J.-P. Monchalin
Industrial Materials Institute, National Research Council Canada, Boucherville, Quebec, Canada

Abstract: The time and Fourier domain Synthetic Aperture Focusing Technique (SAFT and F-SAFT) have been used to improve both sensitivity and lateral resolution of ultrasonic NDT. Following acquisition of signals over the surface of the tested piece, SAFT identifies a defect by summing all the signals within a certain area (the aperture) after giving proper time-delays. F-SAFT, although using the same data, is based instead on the angular spectrum approach and utilizes a backpropagation algorithm to find the field in any plane inside the material. F-SAFT provides an accurate and time-efficient algorithm for 3-D reconstruction. We have introduced several improvements to the F-SAFT algorithm and we have coupled it to laser-ultrasonics. Improvements include temporal deconvolution to enhance both axial and lateral resolutions, control of the aperture to improve signal-to-noise ratio, as well as spatial interpolation in each sub-surface plane. The actual performance of F-SAFT is investigated for imaging simulated and real defects in several applications such as the detection of inclusions in steel slabs, visualization of stress corrosion cracks and delaminations along curved interfaces.

Introduction: Ultrasonic testing is widely used for detecting, locating and sizing flaws in many applications. In conventional ultrasonics, an improvement of the lateral resolution and signal-to-noise ratio (SNR) is achieved by focusing the acoustic field with lenses or curved transducers or by using a computational technique that basically consists of performing the focusing numerically. The last method is known as the Synthetic Aperture Focusing Technique [1]. SAFT is traditionally implemented by scanning a focused piezoelectric transducer over the surface of the specimen and then processing the collected data array. Originally developed in the time domain, SAFT can be advantageously implemented in the frequency domain (F-SAFT). F-SAFT is based instead on the plane wave decomposition of the measured ultrasonic field at the surface (angular spectrum approach) and then utilizes a backpropagation algorithm to find the field in any plane inside the material [2, 3]. F-SAFT provides an accurate and time-efficient algorithm for 3-dimensional reconstruction.

On the other hand, laser-ultrasonics has brought practical solutions to a variety of NDT problems that cannot be solved by using conventional ultrasonic techniques [4, 5]. Laser-ultrasonics uses two lasers, one with a short pulse for the generation of ultrasound and another one, long pulse or continuous, coupled to an optical interferometer for detection. Laser-ultrasonics is a technique that combines the advantages of both optical and ultrasonic sensing. Laser-ultrasonics allows sensing remotely as an optical technique and sensing inside materials as well as on their surface as an ultrasonic technique. The technique features also a large detection bandwidth, which is important for numerous applications, particularly small defect detection and material characterization. Another feature of laser-ultrasonics, particularly useful for testing parts of complex shapes, is the generation of an ultrasound wave propagating at well defined angles, independently of the shape of the part and of the incidence angle of the optical generation beam. However, these very attractive characteristics of laser-ultrasonics are often limited by the relatively poor sensitivity of laser-based detection.

Recently, we have introduced several improvements to the F-SAFT algorithm and we have coupled it to laser-ultrasonics [6, 7]. Improvements include temporal deconvolution to enhance both axial and lateral resolutions, control of the aperture to improve signal-to-noise ratio, as well as spatial interpolation in each sub-surface plane The control of the aperture also allows reduction in the sampling requirements to further decrease both data acquisition time and processing time, therefore making the technique more attractive for industrial use. It should be noted that laser-ultrasonics is inherently well adapted for SAFT data acquisition since laser beams are easily

scanned, far-field ultrasound is easily obtained, and the generated ultrasound is widely diverging. SAFT compensates the relatively poor sensitivity of laser-based detection by collecting and adding up many signals originating from the detected defect. In this paper, we demonstrate the capability of this combined technique for detecting and characterizing flaws in structural materials. The actual performance of F-SAFT is investigated for imaging simulated and real defects in several applications such as the detection of inclusions in steel slabs, visualization of stress corrosion cracks (SCCs) and delaminations along curved interfaces.

F-SAFT method: We assume that the generation and detection beams are focused at the same location onto the surface. By moving the sample mounted on a stage or by scanning the laser beams, a 2-D mesh of signals at the surface of the material is obtained. As shown in Fig. 1, if a diffraction source, such as a defect tip, is present at point C located at a depth z within the sample, this particular point re-radiates the acoustic field originating at point M_j. The ultrasonic signal $S(M_i,t)$ received at any point M_i in the measurement mesh exhibits a peak at time $t = 2d_i / v$, where v is the ultrasonic wave velocity in the material and d_i is the distance CM_i. Consequently, the summation:

$$\Sigma(C) = \sum_{M_i \in mesh} S\left(M_i, t = \frac{2d_i}{v}\right)$$ (1)

separates the points C, where superpositions build up and defects are present, from any other points C, where no coherent superposition occurs. Moreover, the function $\Sigma(C)$ increases the SNR for the detection of defects by the factor $\sqrt{N}$, where N is the number of points M_i in the measurement mesh aperture (the synthetic aperture). It can be shown that the lateral and depth resolutions obtained from the SAFT algorithm are respectively:

$$\Delta x \approx v \cdot \Delta t \cdot \frac{z}{a} \quad , \quad \Delta z \approx \frac{v \cdot \Delta t}{2}$$ (2)

where Δt is the ultrasonic pulse duration and a is the dimension of the synthetic aperture. While maintaining the depth resolution of the conventional pulse-echo method, the SAFT processing leads to improved lateral resolution. In practice, the directivity pattern at generation and the detection sensitivity should be taken into consideration to determine the aperture.
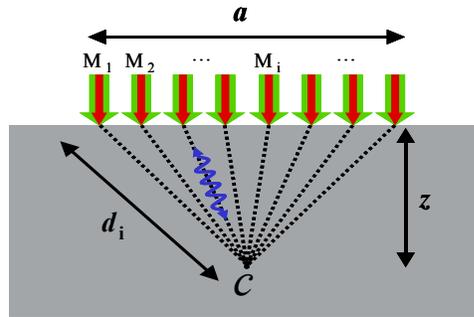

Figure 1: Principle of synthetic aperture focusing technique.

This data processing approach, while straightforward in its principle and implementation, is not very efficient and is very computation intensive. An alternative method is the frequency domain SAFT (F-SAFT) whereby the data processing is performed in the 3-D Fourier space using the angular spectrum method [3, 6]. Starting from the acoustic field $S(x, y, z=0, t)$ at the sample surface of the measurement mesh (axes *x* and *y*), a 3-D Fourier transformation is performed with respect to variables (x, y, t) into a 3-D Fourier space represented by variables (σ_x, σ_y, f).

Physically this consists in representing each acoustic field at f by a superposition of plane waves

at different angles with spatial frequencies σ_x, σ_y. Then, assuming a defect located at depth z, the transformed field $\overline{S}(\sigma_x, \sigma_y, z = 0, f)$ is backpropagated to any depth z using:

$$\overline{S}(\sigma_x, \sigma_y, z, f) = \overline{S}(\sigma_x, \sigma_y, 0, f) \exp\left(\pm 2\pi i z \sqrt{(2f/v)^2 - \sigma_x^2 - \sigma_y^2}\right) \qquad (3)$$

with $\pm$ corresponding to the sign of f and is summed over the temporal frequencies as follows:

$$\overline{\Sigma}(\sigma_x, \sigma_y, z) = \sum_{f \in \Omega} \overline{S}(\sigma_x, \sigma_y, z, f) \qquad (4)$$

where Ω is the selected frequency bandwidth including negative components. Finally, an inverse 2-D Fourier transformation of $\overline{\Sigma}(\sigma_x, \sigma_y, z)$ with respect to variables (σ_x, σ_y) is performed, yielding the space domain function $\Sigma(x, y, z)$. A point C (at position x, y, z) will correspond to a defect if the summation Σ at this point exhibits a peak.

One improvement to this approach is obtained by controlling the aperture in the frequency domain to further improve speed and SNR. As mentioned, the 3-D Fourier transformation can be seen as representing the acoustic field at f by a superposition of plane waves at different angles. The direction cosines of the wave components are related to the orientation of the wave vector, k, with respect to the coordinate axes. Note that for simultaneously scanned generation and detection, the propagation distances are doubled and this results in an effective wave vector augmented by the factor 2 in Eq. (3). Therefore, the angle of a plane wave with respect to the z axis is given by:

$$\frac{k_z}{k} = \frac{\sqrt{(2f/v)^2 - \sigma_x^2 - \sigma_y^2}}{2f/v} = \cos\theta_z \qquad (5)$$

For laser-generated longitudinal waves, the amplitude decreases away from the normal to the surface and one should limit θ_z to a maximum value θ_{max}^L to avoid the addition of noise, i.e. $\cos\theta_z > \cos\theta_{max}^L$. Laser-generated shear waves have an angled emission pattern and one should limit θ_z to both a minimum value θ_{min}^S and a maximum value θ_{max}^S to avoid the addition of noise, i.e. an annular aperture with $\cos\theta_{max}^S < \cos\theta_z < \cos\theta_{min}^S$. Note that introducing a lower limit could also be useful for laser-generated longitudinal waves to reduce direct contribution from the backwall and improve contrast in the image. It then follows the general condition on the temporal frequencies f to be included in the summation of Eq. (4):

$$\frac{v}{2} \frac{\sqrt{\sigma_x^2 + \sigma_y^2}}{\sin\theta_{max}} < f < \frac{v}{2} \frac{\sqrt{\sigma_x^2 + \sigma_y^2}}{\sin\theta_{min}} < f_{max} \qquad (6)$$

where f_{max} is the maximum frequency in the bandwidth Ω. For increasing values of the spatial components σ_x, σ_y, the number of temporal frequency components f used in the summation is progressively reduced. It has been shown for reconstruction with longitudinal waves [7], that the SNR rapidly increases with aperture size, reaches a maximum for θ_{max} of about 30° and then progressively decreases by at least 6 dB, as a result of including components that contributes more to noise than to coherent signal. In addition, the processing time is reduced since less data points are included in the SAFT processing by proper reduction of the aperture. Eq. (6) is an extension of the results reported in Ref. [7]. Other improvements in the implementation of F-SAFT can be found in that reference.

Results: A first application to illustrate the capability of F-SAFT is the detection of inclusions in steel slabs. Although steel industry tries to make very clean steel, the presence of small defects (voids and particular inclusions) in cast slabs is hard to avoid and could lead to a variety of problems down the processing line. These defects are mainly found within a depth of about 10

mm below the surface. A technique for the detection of small defects buried in descaled slabs that combines laser-ultrasonics and F-SAFT processing has been proposed. The laser-ultrasonic system is composed of a Q-switched Nd:YAG laser operated at its second harmonic (λ=532 nm) for generation, with a pulse duration of 10 ns, and a Nd:YAG laser in the fundamental mode for detection (λ=1064 nm), with long pulse duration of 100 µs. The scattered light phase-modulated by the ultrasonic surface motion is collected and sent into the confocal Fabry-Perot interferometer. In this setup, the bandwidth of detection system is between 1 and 12 MHz. The experiments were performed in a pulse-echo configuration, generation and detection lasers impinging at about the same location on the sample surface.

An additional improvement in F-SAFT reconstruction is the correction of the surface profile for the application to steel slab measurements. The surface profile is measured optically using a low coherence interferometry (LCI) technique. For details about the technique, see Ref. [8]. The profile measurement can be made simultaneously or after laser-ultrasonic inspection of the scanned area. From the measured profile, a simple correction method is applied in the first stage of F-SAFT reconstruction prior to processing in the Fourier domain. The surface height ξ is measured at a given location and the actual propagation distance of the ultrasound from the defect at depth z to the detection surface is d_r. In case of an idealized flat inspection surface, the propagation distance to the defect would have been d_i. The first order correction adopted here is to shift each signal according to an approximation of d_i given by:

$$\hat{d}_i = d_r - \alpha(\theta_z)\xi \tag{7}$$

A further approximation, valid for an aperture angle $\theta_{max} < 30^o$ is to consider α constant, minimizing the error over the full aperture, with the value $\alpha \approx 0.95$.

Samples taken from an industrial steel slab and having flat-bottom holes at different depths were tested to validate the approach. These samples were provided by IRSID-USINOR in France. One sample is a 10 mm thick plate that has been descaled. The removal of loose scale at the surface is needed since any air gap or poor contact between the surface oxide and the cast slab will prevent coupling of the ultrasonic wave in the material. To simulate defects, flat-bottom holes of diameters 1 and 2 mm were drilled from the back surface in both samples, at depths of the order of 1 and 5 mm below the inspected surface. Fig. 2 shows a photo of the sample surface and the location of the holes. Notice that an easier case is when the sample surface is descaled and then smoothed by flame. Flaming is usually performed for eddy currents inspection, since the descaled surface is often too rough for this kind of inspection, having peaks and ditches of the order of one mm or more.

The inspection was performed in a scanned area of 28 X 28 mm^2 with a step size of 0.2 mm. The F-SAFT reconstruction was made with the use of the longitudinal wave dominant in the ultrasonic signals, with a velocity v = 6.12 mm/µs. Results for the descaled-only sample are presented in Fig. 3. The figure includes the amplitude C-scans (top) gated at the depth of the holes, and B-scans (bottom) across the holes. In Fig. 3a, the presence of the deepest 1 mm hole is seen in the C-scan (at the intersection of the two cursors), with a depth estimated from the B-scan to be 3.6 mm. The B-scan also shows the 2 mm hole at a slightly different depth. In Fig. 3b, the C-scan shows the presence of the 1 mm hole near the surface and the depth estimated is about 0.9 mm by considering the strongest amplitude among the multiple reflections observed in the B-scan. Also not shown here, we have identified the presence of a few natural defects at various depths in both samples. An important concern about the inspection of steel slabs is the scanning step size required. As reported in Ref. [7], the control of the aperture in the F-SAFT processing allows a reduction in the sampling requirement for data acquisition and processing. It is shown that a step size of nearly 1 mm would be sufficient to detect the 1 mm holes detected above. However, the inspection time in a real situation is still quite large when considering smaller defects. Therefore, a statistical approach, where only randomly selected areas on the steel slab are inspected, can only be considered in practice.
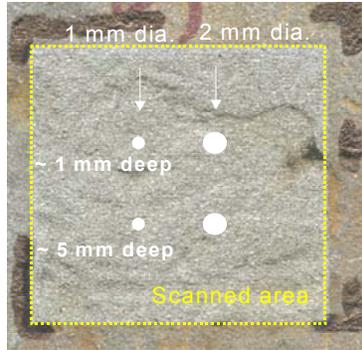
Figure 2: Surface of only-descaled sample and locations of the holes drilled from the back surface.
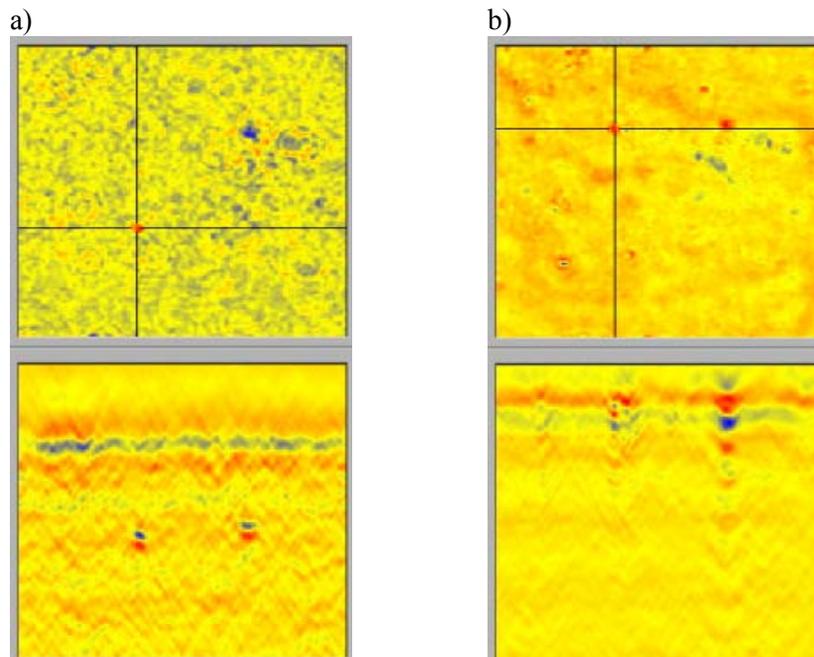

Figure 3: C-scan (top) and B-scan (bottom) for the descaled-only sample, with the 1 mm holes at a depth of 3.6 mm in a), and near the surface at 0.9 mm in b).

A second application is the visualization of stress corrosion cracks (SCCs) using laser-ultrasonics. Ultrasonic waves are generated by Q-switched Nd:YAG laser pulses (λ=532 nm), of pulse duration 10 ns. A lens is used to focus the laser pulses onto the sample surface with a diameter of about 100 µm producing slight ablation at each irradiated spot. This method simultaneously generates bulk longitudinal waves (L) and shear waves (S) with frequencies typically between 0.5 MHz and 20 MHz and having their respective directivities. The ultrasonic waves travelling in the medium are detected by measuring the displacement of the sample surface using a confocal Fabry-Perot interferometer. The detection laser is a Nd:YAG laser (λ=1064 nm) emitting long pulses. The tested samples provided by Toshiba Corp. in Japan were made from 100 mm (L) x 50 mm (W) x 10 mm (D) stainless steel plates and contained a few stress corrosion cracks. These SCCs, each typically less than 0.05 mm wide and from 0.5 to 5 mm deep, were produced by boiling the plate in a $MgCl_2$ solution with applied stress. The samples were interrogated from a surface opposite to the cracking with the generation and detection nearly superimposed.

The step size of the scan was 0.2 mm and the scanned area was about 40 x 40 mm^2. The data were processed using the F-SAFT algorithm. The aperture angles used were from 5° to 25° for the L-wave reconstruction and from 35° to 55° for the S-wave reconstruction. It is noted that the contributions from 0° to 5° for the L-wave were omitted because near-normal bottom echoes have much stronger amplitudes and sometimes reduce the contrast of the defect-related indications on the reconstructed images. C-scans acquired on one sample and reconstructed by using both L-wave and S-wave velocities are compared to the images by liquid penetrant testing (PT) in Fig. 4. Each C-scan was obtained by selecting the peak-to-peak value from each A-scan in a narrow gate at depths corresponding to the cracking surface. It is found that F-SAFT provides very fine images of the surface which contains SCCs, from inspection on the opposite side. The detectability of detailed structures of F-SAFT can exceed that of PT, which is considered the most sensitive method to visualize fine cracks. When comparing the processed images using L-wave (F-SAFT(L)) and S-wave (F-SAFT(S)), the SNR of F-SAFT(L) is slightly better than that of F-SAFT(S). However, the spatial resolution of F-SAFT(S) is higher than that of F-SAFT(L). Reconstructed B-scans nearly vertical to SCCs by using L-waves and S-waves are shown in Fig. 5. The image reconstructed with L-waves shows the crack roots as a lack of signal having a width not well defined. The image with S-waves shows a feature having a cross-like shape ("X" shape), the center of which has the maximum amplitude and is located at the position of the crack root on the cracked surface. This feature using F-SAFT(S) provides the excellent crack opening images shown in Fig. 4.
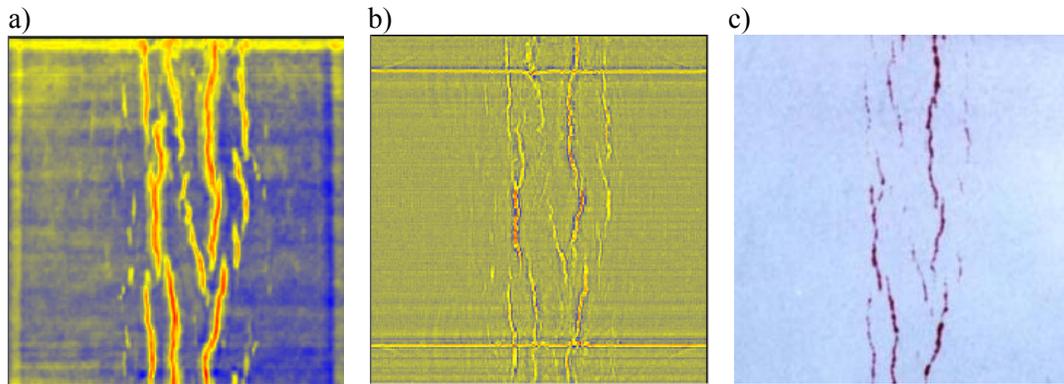
a)   b)   c)

Figure 4: C-scans of the cracking surface on a SCCs sample using a) F-SAFT(L), b) F-SAFT(S) and c) PT.
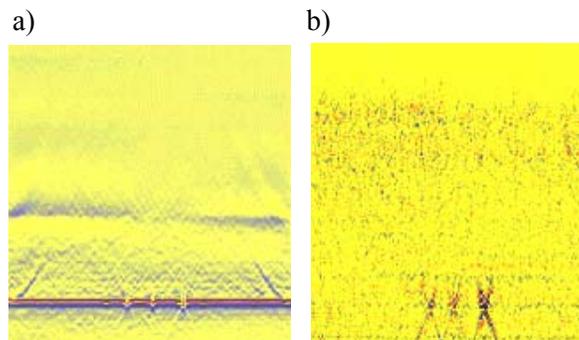
a)   b)

Figure 5: Typical B-scans on SCCs samples using a) F-SAFT(L), b) F-SAFT(S).

The "X" shape appears related to the existence of a corner near the crack root and one may wonder if its dimension, in particular its length, is related to crack depth. Measurements carried out on an artificial slot having a variable depth from 0 to 3 mm showed that the length of the "X"

shape is nearly constant, independent of the slot depth and that the amplitude at the cross point relates to the depth. This means that the color variations in the C-scans for F-SAFT(S) in Fig. 4 can be related to the depths of those cracks. This was also confirmed by simulations based on time-domain SAFT when predicting the locus drawn by the imaginary diffraction points. Therefore, the "X" shape feature is very useful for visualizing cracks from the opposite side. A remarkable aspect is that the presence of the "X" shape is a particular feature that only laser-generated S-waves can produce. To form the indication, two symmetric angled lobes of ultrasound emission are required. Emission patterns of laser-generated L-waves are essentially normal and angled beams produced by the conventional method are not symmetric with respect to the surface normal. Laser-generated S-waves, which typically have two lobes angled -45° and +45°, is well adapted to form the "X" shape and visualize the fine surface image of tight cracks.

A third application is visualization of delaminations along curved interfaces also using laser-ultrasonics. An example is Mg/Al castings currently under evaluation by an automotive industry manufacturer for fabricating engine parts. In a typical Mg/Al casting part, the Mg/Al interface is not parallel to the top Mg surface. It follows that the ultrasonic wave can be reflected obliquely from the Mg/Al interface to any location on the Mg surface surrounding the generation point. Then, the small ultrasonic displacement of the Mg surface will not be properly detected unless the detection laser spot is either at the right location, or the detection laser spot is large enough. A better approach is to process the data with F-SAFT, therefore allowing synchronization of the ultrasonic signals scattered back in different directions from each point of the Mg/Al interface. A testpiece of Mg/Al casting provided by Noranda Inc. in Canada is shown in Fig. 6, composed of an Al core enclosed in a Mg shell. Eight flat bottom holes (two lines of holes with the following diameters: 10, 5, 1, 0.5 mm) have been drilled in the Al part to simulate delaminations. These flat bottom holes have a depth such that the bottom of the hole is located at the interface of the two alloys. The inspection has been performed from the Mg shell surface in an area of 40 x 15 mm^2 of the testpiece. The laser-ultrasonic scans parameters for using F-SAFT processing were: 0.3 mm diameter spot size for the Nd:YAG generation laser, 0.2 mm diameter spot size for the long pulse Nd:YAG detection laser, 0.2 mm scanning step size and a frequency bandwidth between 1 and 20 MHz.

Figure 6: Mg/Al testpiece with flat bottom holes of diameters 10, 5, 1 and 0.5 mm. The dashed rectangle indicates the inspected area for SAFT processing.

Fig. 7 shows F-SAFT images obtained from scanning the testpiece where the Mg/Al interface is non-parallel, as indicated in Fig. 6. Fig. 7a and Fig. 7b are C-scans taken at depths of 8.2 and 9.7 mm respectively. Fig. 7c is a B-scan which shows the curved Mg/Al interface as well as the depth of the two C-scans. In Fig. 7b, the two flat bottom holes of diameters 10 and 5 mm included in the scanned area are observed at a depth of 9.7 mm where the interface is almost flat and parallel to the scanned surface. In Fig 7a, corresponding to a depth of 8.2 mm, a horizontal line of variable amplitude (yellow to red) is observed. This line is the intersection of the curved Mg/Al interface with the observation plane (parallel to the scanned surface). Along this intersection line, we believe that the regions in red are indicative of a delaminated area.
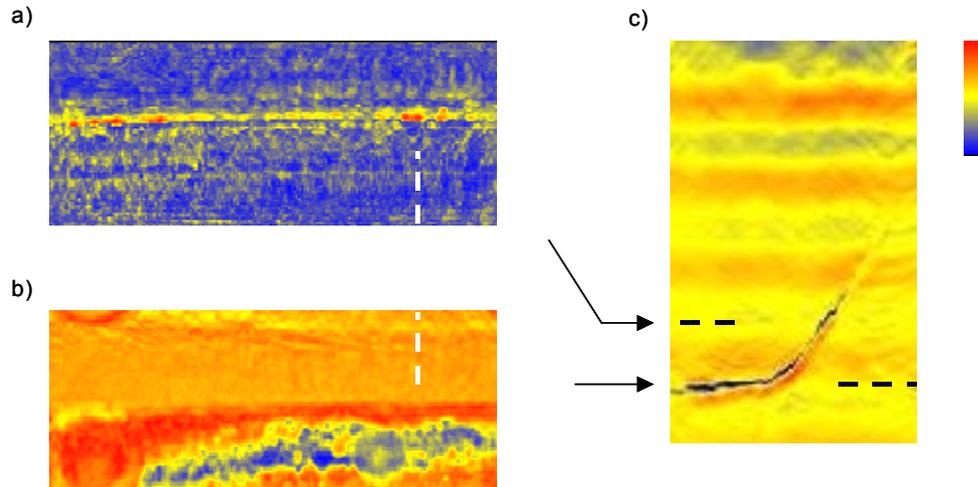
Figure 7: SAFT images of the Mg/Al testpiece in a region having Mg/Al interface non-parallel to the surface. The C-scans a) and b) have depths indicated in the B-scan c). The B-scan is at position indicated in a) and b).

Conclusions: We have demonstrated the capability of laser-ultrasonics combined with 3-dimensional F-SAFT reconstruction for detecting and characterizing flaws in structural materials. The actual performance of F-SAFT is reported for imaging defects in three industrial applications relating to detection of inclusions in steel slabs, visualization of stress corrosion cracks and delaminations along curved interfaces. In particular, surface images reconstructed by F-SAFT(S) can surpass results of the conventional PT in visualizing the detailed structure of surface-breaking tight cracks. It should be noted that these results also depend on several characteristics of laser-ultrasonics. Laser-ultrasonics is not only a technique of interest for the non-contact and/or remote inspection but also offers many attractive features, such as: 1) ultrasonic far-field is easily obtained, 2) wide bandwidth and widely diverging ultrasound can be used, 3) low frequency ultrasound is available even when the generation spot is very small, 4) small laser spots allow high spatial and temporal resolutions, and 5) complex shapes can be scanned easily.

References:
[1] Doctor, S. R., et al., "SAFT - the Evolution of a Signal Processing Technology for Ultrasonic Testing," *NDT-International* 19, 1986, pp. 163-167.
[2] Mayer, K., et al., "Three-dimensional Imaging System Based on Fourier Transform Synthetic Aperture Focusing Technique," *Ultrasonics* 28, 1990, pp. 241-255.
[3] Busse, L. J., "Three-Dimensional Imaging Using a Frequency-Domain Synthetic Aperture Focusing Technique," *IEEE Transactions on Ultrasonics, Ferroelectrics, and Frequency Control* 39, 1992, pp. 174-179.
[4] Scruby, C. B. and L. E. Drain, "Laser-ultrasonics: Techniques and Applications," Bristol, Adam Hilger, 1990.
[5] Monchalin, J. -P. et al., "Laser-ultrasonics: from the Laboratory to the Shop Floor," *Advanced performance materials* 5, 1998, pp. 7-23.
[6] Blouin A., et al., "Improved resolution and signal-to-noise ratio in laser-ultrasonics by synthetic aperture focusing technique (SAFT) processing", *Optics Express* 2, 1998, pp. 531-539.
[7] Lévesque, D., et al., "Performance of Laser-Ultrasonic F-SAFT Imaging," *Ultrasonics* 40, 2002, pp. 1057-1063.
[8] Danielson, B.L., Boisrobert, C.Y., "Absolute optical ranging using low coherence interferometry", *Appl. Optics* 30, 1991, pp. 2975-2979.